BRCORP
TECHNOLOGY | INNOVATION | INDUSTRY

*International Journal of*
*Advanced Structures and Geotechnical Engineering*
*ISSN 2319-5347, Vol. 03, No. 04, October 2014*

# Application of sodium silicate-cement grout to enhance the liquefaction resistance and dynamic properties of sandy soil

**TO ANH VU PHAN**
*Department of Civil Engineering, National Kaohsiung University of Applied Sciences, Taiwan*
*Email: phantoanhvu@yahoo.com*

**Abstract:** The article aims to present an experimental dynamic behavior of grouted sand. Two different base gradations of between the Nos. 4 and 40 sieve sizes (4/40) and between the Nos. 40 and 100 sieve sizes (40/100) were mixed with different ratios. Three different ratios of sodium silicate-cement grout (0%, 7%, 14%), by volume, were permeated to mixed sample. The specimens were allowed to cure after 3 and 14 days. The cyclic triaxial test found that the grouted-sand significantly enhanced the liquefaction resistance. Also, the cyclic stress ratio-grout content relation can be analytically expressed in an exponential function with a highly reliable ($R^2 \geq 0.96$). Resonant column test showed that shear modulus non-linearly decreased as shear strain increased, and increased with increasing the grout content and confining pressure. For damping ratio, the result of grouted sands was greater than that of non-grouted sand with the amplitude of strain in range of 0.001% and 0.1%; however, with the amplitude of strain greater than 0.1%, result of non-grouted-sand was greater than that of grouted-sand.

***Keywords:*** *Sodium silicate, Cement, Liquefaction resistance, Shear modulus, Damping ratio*

## 1. Introduction:

Over the three past decades, soil liquefaction is one of the most interesting and complex phenomenon during seismic loading of earthquake. This is most frequently related with cohesionless soils in which increases in pore pressure and reduces the effective confining pressure. The result is to suddenly decrease the shear modulus of the soil, which in turn, results in increasing soil deformation, a loss in bearing strength. In the case of full liquefaction, when increasing pore water pressure reduces the effective stress to zero, the soil experiences a full loss of strength and undergoes large viscous deformations.

To mitigate the liquefaction risk, the usage of remedial measures probably the only available option for many existing structures that have been constructed in the liquefiable soil areas. In practice, chemical grouting can be undertaken to mitigate the liquefaction [1] and also may be one of the most effective methods. In general, poor soil conditions can be significantly improved the physical and engineering properties by chemical grouting technique, such as strength, hydraulic conductivity, volume stability, stiffness, undrained shear strength which related with liquefaction potential. Furthermore, the widespread use of grouting method demands a profound understanding of characteristic and behavior of grouted materials including dynamic properties.

So far, some chemical grouts were popularly used such as cement-, micro-fine cement-, sodium silicate-, colloidal silica-, mineral-grout. With regard to cement grout, although less dynamic than static tests of cemented soil properties, the literature reviews showed that ordinary Portland cement was used to improve significantly the liquefaction resistance as well as stiffness of soil [2-7].

For micro-fine cement grout, it first appeared in Japan about 30 years ago and has become commonly available. The advantage of this material is not only better flow properties and bleed charateristics than that of ordinary Portland cement grout, but also permeates easily medium-to-coarse sands [8, 9]. Maher (1994) [1] described that the micro-fine cement caused the sand not to experience any initial liquefaction or 5% cyclic mobility for the ranges of stress ratio and cyclic numbers test. Delfosse-Ribay et al. (2004) [10] revealed that micro-fine grouting improve the stiffness with the factor of 4 times larger. Pantazopoulos et al (2012) [11] draw a conclusion that micro-fine cement grouted sands obtain higher shear modulus, initial Young's modulus and damping ratio values than sands grouted with ordinary cements, by 25%–40%.

Certain results showed that the usage of colloidal silica grouted sand substantially improve the liquefaction potential and cyclic undrained behavior of loose sand [12]. Similarly, Liao et al. (2014) [13] employed the colloidal silica as grouting material to improve the liquefaction resistance of in-situ soil sandy soil. Test results showed that up to 4 ~ 7 folds increased in liquefaction resistance of grouted sand compared with that of ungrouted sand was obtained. Higher stress ratio and more number of loading cycles were needed to initial in grouted sand specimens. Especially, the sand stabilized with colloidal silica grout significantly increase unconfined compression strength [14, 15].

Sodium silicates have been developed into variety of different systems and widely using as a chemical grout. The sodium silicate systems consist of sodium silicate and a hardener which can be used effective to get the strong bonding properties in two-compound system [16]. The results of dynamic of dynamic properties still were limit [3, 10, 17, 18]. Tsai et al. (2013) [3] presented the result of an experimental comparing the sodium silicate – cement stabilized soil with cement stabilized soil and slag cement stabilized soil. The results indicated that maximum shear modulus of cement stabilized soil increases with increasing confining pressure, the minimum damping ratio decreases with increasing confining pressure, the sodium silicate – cement stabilized soil was able to sustain larger shearing strain before stiffness degradation occurring than other types of additive.

The aim of study presents experimental results in laboratory to find the engineering dynamic properties of sodium silicate-cement sand mixture. After permeating grout to specimen, the cement content was calculated as 1% and 2% by weight. A series of cyclic triaxial tests were conducted to investigate the improvement of liquefaction resistance. Also, shear modulus and damping ratio were determined using resonant column test. Finally, the effects of grout content, curing age, confining pressure, and shear strain on liquefaction resistance, shear modulus and damping ratio were discussed in this study.

## 2. Material used:

### 2.1. Sand mixtures:

The natural soil used in this experimental investigation was taken from the Li-Gang river shore, Pingtung county, located in Kaohsiung city, Taiwan. Two different base gradations of sand were produced. They consisted of gradations between the Nos. 4 and 40 sieve sizes (4/40) (4.75-0.425 mm), namely medium sand MS; and between Nos. 40 and 100 sieve sizes (40/100) (0.425-0.15 mm), namely fine sand FS.

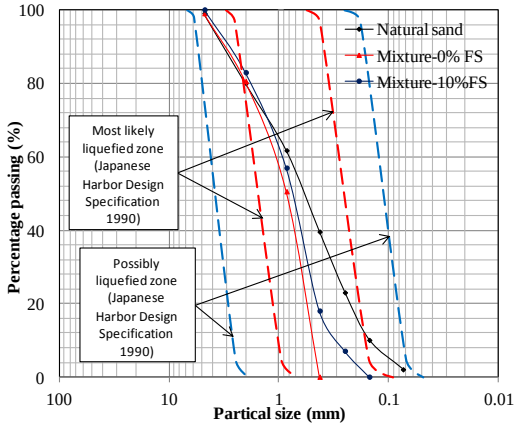


*Figure 1: Grain size distribution of natural sand, sand mixtures*

The first series of the test was prepared with 2 various mixtures by dry weight: 100% MS plus 0% FS, which was named by A; 90% MS plus 10% FS, which was named by B. Based on ASTM D422, the grain size distribution curve for all of sand mixtures are also described in Fig. 1. According to Japanese harbor design specification (1990), the grain size distributions of different sand mixtures located in range of most likely to liquefy or possible liquefied zone. Specific gravity test was conducted in accordance with ASTM D854 and yielded the value $G_s$ of 2.69. Both ASTM D4253 and ASTM D4254 were used to test the maximum density, and minimum density. The properties of sand mixtures were presented in Table 1.

Table 1: Index physical properties of sand mixtures

| **Tests** | **Sand mix.** | |
|---|---|---|
| | **FS=0%** | **FS=10%** |
| Specific gravity, $G_s$ | 2.69 | 2.69 |
| Uniformity coefficient, $C_u$ | 2.2 | 3.03 |
| Coefficient of gradation, $C_c$ | 0.72 | 0.96 |
| Unified soil classification System , USCS | SP | SP |

### 2.2. Sodium silicate - cement grouting (SSC):

Sodium silicate-cement grout is the mixture of chemical combination of sodium solution and cement solution. The usage of this mixture takes the several advantages such as reliable, proven performance, safety, environmental acceptability, and low-cost. The initial and final setting time for SSC grouting is 270 minutes and 1100 minutes, respectively. Two types of solutions are denoted by solution A and B. Sodium silicate, used for solution A, the silicate grout composed of water and sodium silicate. The water to sodium silicate ratio in volume is 1:4. The molecular ratio (Rp = $SiO_2/Na_2O$) is equal to 3 or greater. The Sodium silicate used in this study was manufactured by Pinnacle Industrial Co. Ltd. The chemical contents of sodium silicate are reported in the table 2.

Table 2: The chemical ingredient for solution A

| $SiO_2$ (%) | $Na_20$ (%) | Moisture (%) | Fe (%) | Insolubility (%) |
|---|---|---|---|---|
| 28.8 | 9.17 | 64.2 | 0.012 | 0.072 |

Ordinary Portland cement (type 1) is for solution B, the cement grout was contained by water and cement. The chemical contents and basic physical properties are presented in Table 3 and Table 4, respectively.

Table 3: Chemical content of OPC (%)

| $SiO_2$ | $Al_2O_3$ | $Fe_2O_3$ | CaO |
|---|---|---|---|
| 21.24 | 4.44 | 3.44 | 64.51 |
| MgO | $S0_3$ | $Na_2O$ | $K_2O$ |
| 2.35 | 2.10 | 0.18 | 0.59 |

Table 4: OPC physical properties

| **Ingredient** | **values** |
|---|---|
| Specific gravity | 3.16 |
| Fineness ($cm^2/g$) | 3490 |
| Loss on Ignition (%) | 0.98 |
| Insolubility (%) | 0.12 |
| Alkali content (%) | 0.57 |
| Initial setting time (min.) | 139 |
| Final setting time (min.) | 255 |

In this study, SSC grout consisted of solution A and solution B with the ratio in volume was 1:1. After finishing the infection to the specimen, the SSC grout was filled up with 1% (SSC-1), 2% (SSC-2) cement content by weight, respectively. The pure sand was denoted SSC-0. The grout volume needed for each specimen was presented in Table 5. It is noticed that the 600ml is approximately 2.5 times larger than the void volume of each sample.

Table 5: Grout composition

| Type grout | Solution A (300ml) | | Solution B (300 ml) | |
|---|---|---|---|---|
| | Sodium silicate (ml) | Water (ml) | Cement (g) | Water (mml) |
| SSC-1 | 50 | 250 | 22.6 | 292 |
| SSC-2 | 50 | 250 | 45.2 | 285 |

**3. Specimen preparation:**

Testing process includes the following steps:

-The diameter and height were 7.0 cm and 15.0 cm in height, respectively. The specimen was prepared by wet tamping method. For sample preparation, medium dry sand and fine dry sands have been mixed with respect to the considered different weight ratio (i.e., 0% FS, 10% FS). To obtain the specimen with the relative density of 30 ± 2%, the oven-dry mixture is divided in 5 equal deals, every deal is added some de-aired water to mix to the wet mixture with the exact water content equals to 8%, by weight. Finally, to prevent the grains separation, the specimen was set up in the tri-axial apparatus using mould for rubber membrane, the same initial dry densities were kept during the test process.

- The specimens were allowed to permeate through the specimen from the bottom and overflow from the top with a volume of de-air water 3.0 times the pore volume of specimen. The grout mixture was sequentially injected to the specimens with the volume equal 2.5 times the void volume of the sand specimen.
- After twenty four hours, the specimen was dismantled from the mold, and put in plastic bag and cured in water until testing. All the specimens were conducted on cyclic triaxial and resonant column tests at the age of 3, 14 days.

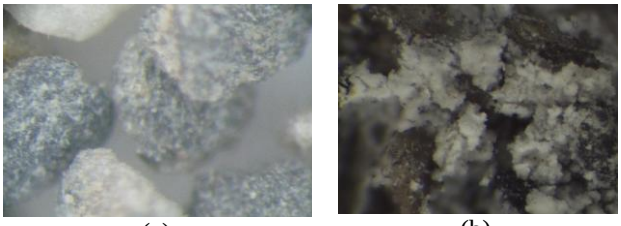

(a) (b)

*Fig. 2 (a) Clean sand (b) grouted sand, magnify X600*

**4. Experimental procedure:**

The experimental test program can be divided into two parts: the first was to determine the cyclic stress ratio; the second was to find the shear modulus and damping ratio of sodium silicate - cement grouted sand.

**4.1. Particle analysis:**

The particle surface analysis was carried out on an optical electron microscope EOM (Environment optical microscope) to understand the different microstructure between the un-grouted and grouted sand, as shown in Fig. 2. It was clear from the Fig. 2a that the un-grouted sand included round spherical shape particle and surrounded with the void; the grey grain was seen in the this type, and there was most unlikely to interconnect between the particles. On the other hand, the grouted sand showed that the surface of particle was covered by white layer surrounding the sand particle, as shown in Fig. 2b.

**4.2. Cyclic triaxial test:**

After completed sample curing, the specimen was consequently saturated by flowing carbon dioxide $CO_2$ at least 60 minutes and then de-aired water was allowed through the specimen from the bottom to the top in order to make sure that the Skempton's coefficient B was equal to or greater than 0.95 at the end of the saturation stage. In this study, backpressure of 200 kPa has been applied during the test to reach the saturation state. After the saturation process, the specimens were objected to the confining pressure for consolidation. During consolidation, the difference between confining pressure and backpressure has been set up so that for each sample the effective consolidation pressure was fixed as 100kpa. The SSC-0, SSC-1, SSC-2 grouted sands were performed on cyclic triaxial test with various fine sands of 0% and 10% FS at the curing time of 3, 14 days.

Cyclic triaxial test was conducted in KUAS's Laboratory in accordance with ASTM D5311, which used the automatic tri-axial test system. During cyclic axial loading, a sinusoidal loading was applied to the saturated specimens with frequency of 1Hz. Variations of excess pore water pressure, axial stress, and axial strain of specimen were recorded during the testing. The loading amplitude was characterized in terms of cyclic stress ratio (CSR) which was defined as

maximum peak shear stress ($\sigma_d/2$) divided by the initial effective consolidation stress ($\sigma_c$).

$$CSR = \frac{\sigma_d}{2\sigma_c} \quad (1)$$

**4.3. Resonant column test:**

SSC-0, SSC-1, SSC-2 grouted sand were tested on the resonant column test to find the shear modulus (G) and damping ratio (D) with the shear strain range of 1% to $10^{-4}$%. For reasons of comparison, the grouted sand containing 0% and 10% FS was tested at curing age of 3, 14 days. In order to investigate the strain range, three types of confining pressure (50, 100 and 200 kPa) were applied on each specimen.

Resonant column test was also known as the Stokoe torsional shear/ resonant column device. The device is a fixed-free system consisting of a cylindrical specimen which has platens attached to each end. During resonant column test, a sinusoidal vibration excitation device with the frequency from 2Hz to 60Hz as applied to the top of specimen. The above testing description corresponds to a cyclic torque of constant amplitude and varying frequency being applied to the top of the specimen. Variations of the peak torsional displacements with varying frequency are recorded to obtain the frequency response curve. The resonant frequency corresponding to the peak of the curve is then obtained. Dynamic soil properties such as small-strain shear modulus G and damping ratio D can be obtained from the resonant frequency, and the frequency response curve.

**5. Results and discussion:**

**5.1. Cyclic triaxial test:**

Fig. 3 presented the cyclic tress ratio (CSR) versus number of cyclic loadings relation. The cyclic triaxial test was carried to evaluate the effect of grout content, fine sand content, curing period on the cyclic stress ratio (CSR), pore water pressure (PWP) and deformation of the specimen. In order to estimate the liquefaction of an earthquake with the magnitude of 7.5, the cyclic stress ratio was defined at 15th number of cyclic. The following the results were presented CSR value versus number of cyclic of 15. The initial liquefaction is defined as the number of cycles required where the excess pore water pressure reached the value just equal to the effective confining pressure and 5% double amplitude axial strain whichever is earlier.

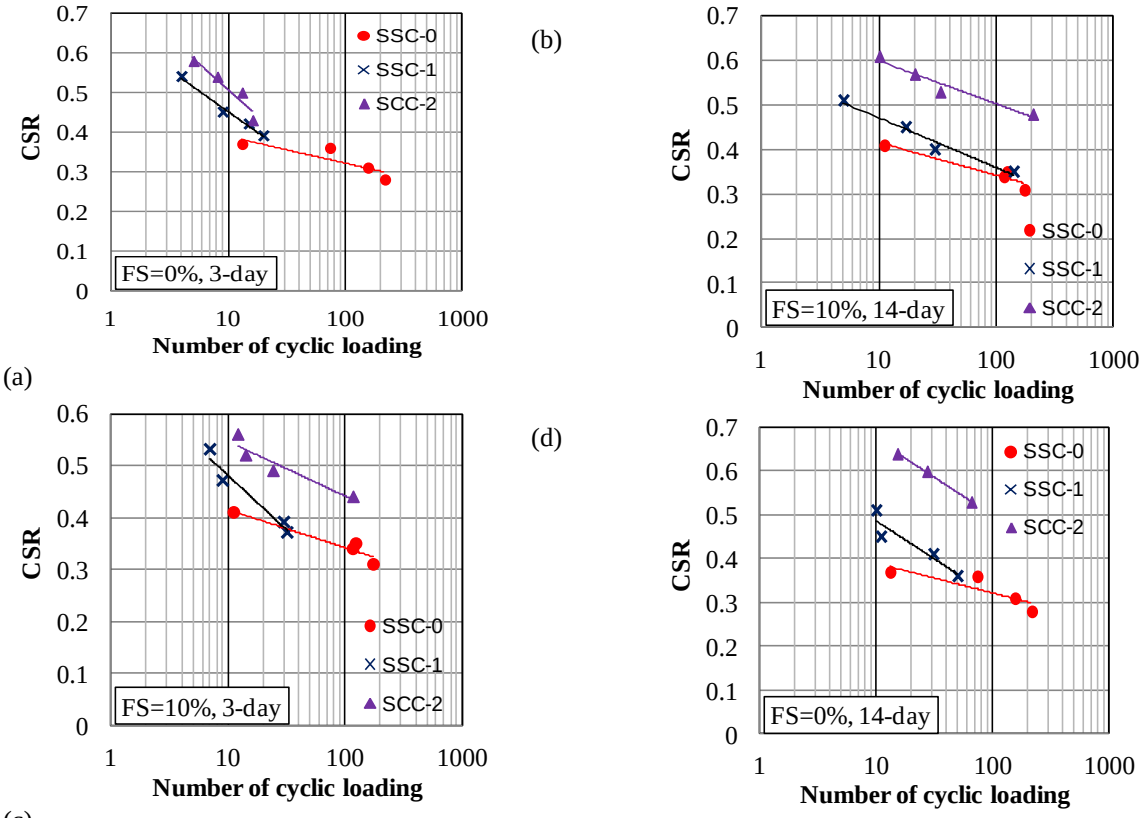


*Fig. 3. Initial cyclic tress ratio (a) 0% FS at 3 days curing (b) 0% FS at 14 days curing (c) 10% FS at 3 days curing (d) 10% FS at 14 days curing*

**5.1.1. Effect of fine sand contents on liquefaction resistance:**

Fig. 4 shows the results between the CSR and fine sand content for different types of grout. For non-grouted sand, the presence of fine sand increases the liquefaction resistance. For instance, The CSR of sand mixture with 0% FS and 10% FS are 0.38 and 0.40, respectively. This is likely attributed to the good grading curve of sand mixed with fine sand. The good grading aggregate slowly make the buildup of excess pore water pressure which can lead to very large deformation as well as increasing the strength and stiffness of the soil. Similarly, for 3-day grouted sand, fine sand increases the liquefaction resistance for both SSC-1 and SSC-2, as shown Fig. 4(a). Otherwise, for 14-day grouted sand, the fine sand decreases the liquefaction resistance for both SSC-1 and SSC-2, as shown in Fig. 4(b). Two different tendencies of CSR are thought as following manner: The fine sand plays an important role in the mixture at the early curing age of 3-day because sodium silicate delays the hydration of cement; when the curing time increases, the grout significantly takes the effect on the liquefaction resistance of mixture, and the larger particle has greater liquefaction resistance than that of smaller particle.

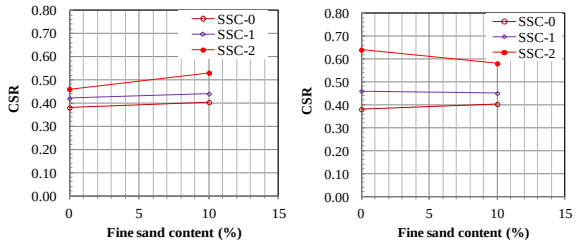


*(a) 3 days* *(b) 14 days*

*Fig. 4. Relationship between CSR and find sand content*

**5.1.2. Effect of grout content on liquefaction resistance:**

It is essential to compare the liquefaction resistance between un-grouted and grouted sand; and the ratio of cyclic stress ratio was , therefore, defined as the rate of cyclic stress ratio of grouted sand relative to that of clean sand.

$$CSR\ Ratio = \frac{Cyclic\ stress\ ratio\ of\ grouted\ sand}{Cyclic\ stress\ ratio\ of\ clean\ sand}$$

Fig. 5 presents the relationship between the CSR ratio with different grout contents. In compared to non-grouted sand, all groups have the average increase of CSR ratio of 1.13-1.21 for 7% grout, and 1.45-1.68 for 14% grout content. As expected, the more grout content has greater CSR value due to continuation of high cementitious-hydrated process. The CSR ratio-grout content relation can be analytically expressed in an exponential function as follow (Eq. [2]):

$$y = a.e^{bx} \qquad (2)$$

where a, b are experimental coefficients; x is grout content; e is Euler's number

The R-squared values were found to be equal or greater than 0.96, and this strongly confirms that the exponential formula are highly reliable for describing liquefaction resistance of the sodium silicate-cement grouted sand.

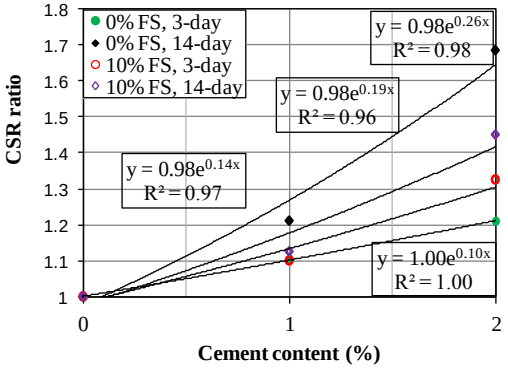


*Figure: 5 Relationship between CSR and grout content*

**5.1.3 Effect of curing time on liquefaction resistance:**

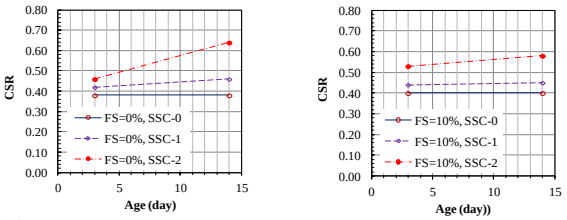


(a) Group A (a) Group B

*Fig. 6. Relationship between CSR and curing age*

**5.1.3 Effect of curing time on liquefaction resistance:**

(a)Group A (b) Group B

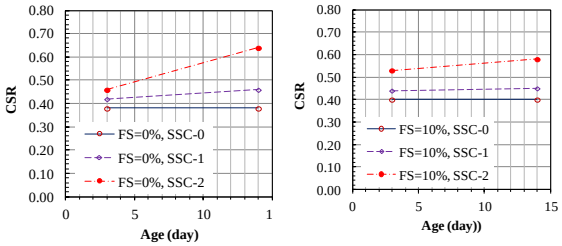


*Fig. 6. Relationship between CSR and curing age*

Fig. 6 shows the relationship between CSR and curing age. As expected, a longer age of curing is a higher CSR due to due to the hydration by sodium silicate and cement to cause the strength and stiffness on the particle of sand. The group A has higher tendency of increasing of CSR than group B. For example, when curing age increases from 3- to 14-days, up 0.46 to 0.64

in CSR for group A, and up 0.53 to 0.58 in CSR for group B. Although group A has greater CSR than group B at early curing age, the CSR value is contrary at the curing age of 14-day. A good reason of this phenomenon was that mixture used sodium silicate reduced the delay of hydraulic reaction of cement particle at an early stage, osmotic bursting of cement was delayed, and the strength was delayed [19, 20]; on the other hand, at the later stage, the porosity of cement with sodium silicate was up to five times greater.

**5.1.4 Discuss on axial strain and pore water pressure:**

Fig. 7 and Fig. 8 show the typical axial strain- and PWP- number of cyclic loading for CSS-0 and CSS-2, respectively. Other groups are not presented due to the same tendency. As clearly seen Fig. 7(b), under a constant cyclic vertical load application pore water pressure rapidly reaches a nearly half value of initial confining pressure at cycle 1 and then gradually increase until cycle 11 where the excess pore water pressure just equal to the effective confining pressure. In addition, Fig. 7(a) shows that small cyclic deformations are induced in specimen until approximately cycle 7, afterward the cyclic deformation builds up rapidly. The increasing axial strain mainly occurs on the negative side.

Similarly, Fig. 8(b) shows the PWP for SSC-2, the under a constant cyclic vertical load application pore water pressure rapidly reaches a half value of initial confining pressure at cycle 1 and then gradually increase until cycle 65 where the excess pore water pressure just equal to the effective confining pressure. Compared to axial strain between Fig. 8(a) and Fig. 7(a), the grouted sand has much more number of cyclic loadings to reach criteria deformation than non-grouted sand, and no positive deformation is obtained. The axial strain of SSC-2 gradually increases with cyclic loadings and build up rapidly the deformation until cycle 75.

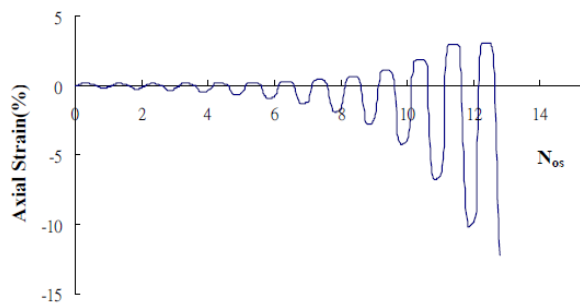


*(a) Axial strain-number of cyclic loading*

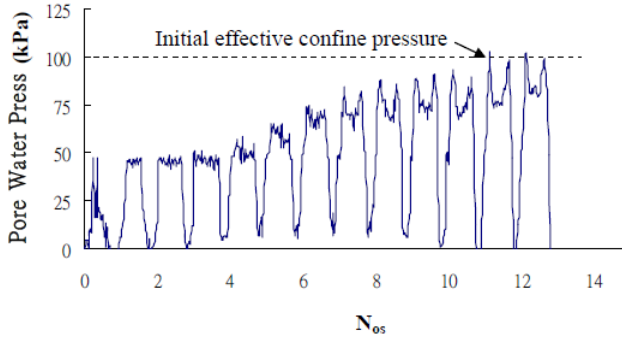


(b) PWP-number of cyclic loading

*Fig. 7. Strain and PWP versus number of cyclic loading of CSS-0, FS=10%, CSR=0.41*

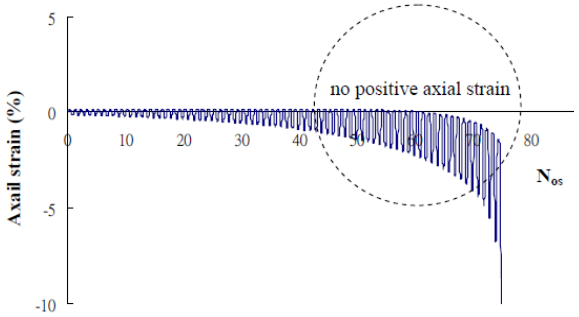


(a) Axial strain-number of cyclic loading

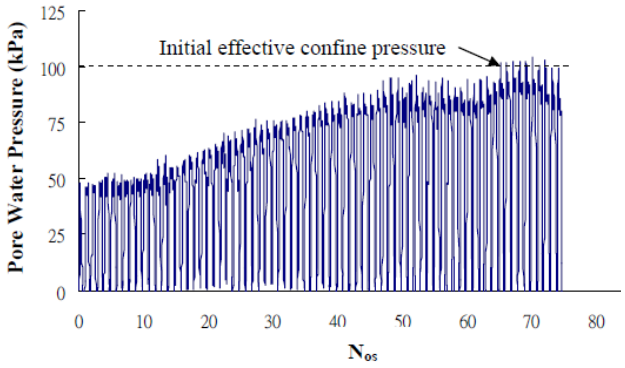


(b) PWP-number of cyclic loading

*Fig. 8. Strain and PWP versus number of cyclic loading of CSS-2, FS=0%, 14-day, CSR=0.53*

**5.2. Resonant column test:**

**5.2.1. Shear modulus:**

The results of variation of shear modulus and shear strain with different grout contents are shown in Fig. 9. In general, the typical results show that the shear modulus decreases with the increase in shear strain. The decrease tendency in shear modulus is due to the nonlinear behavior of sand and grouted sand. The loss of stiffness of mixtures is likely attributable to the weakening of the structure between particle and grout. The phenomena can be explained that the worsening bond between the grains of sand particle and grout

occurs as shear strain increases. In particular, it should be noted that for the shear strain less than $5x10^{-4}$(%), the shear modulus seems to remain the constant value, thus, the maximum shear modulus can be determined by this range of strain. As expected, the greater grout content has greater shear modulus due to the cementituous-hydrated process. Also, higher confining pressure yield the greater shear modulus due to the strengthening of stiffness.

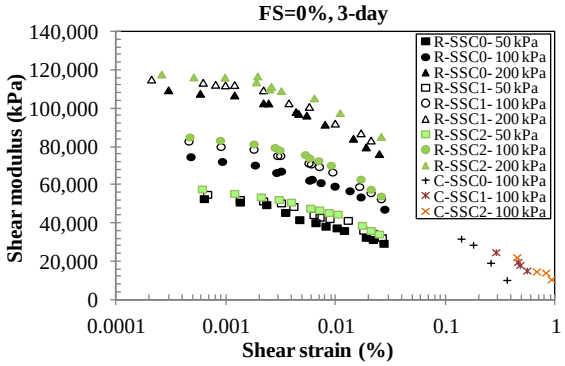


(a) FS=0%, 3-day

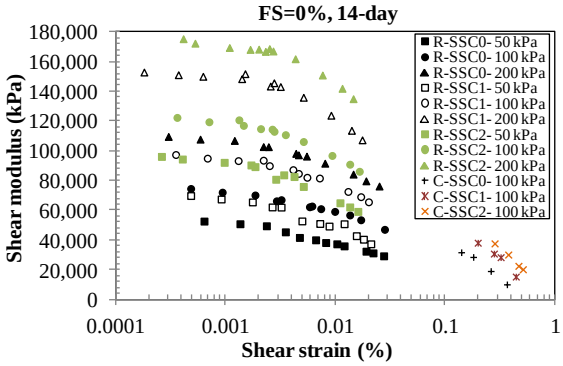


(b) FS=0%, 14-day

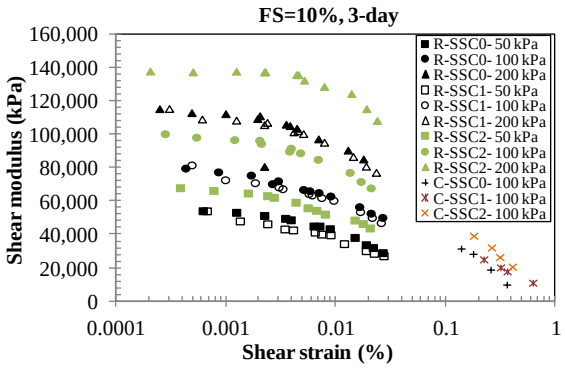


(c) FS=10%, 3-day

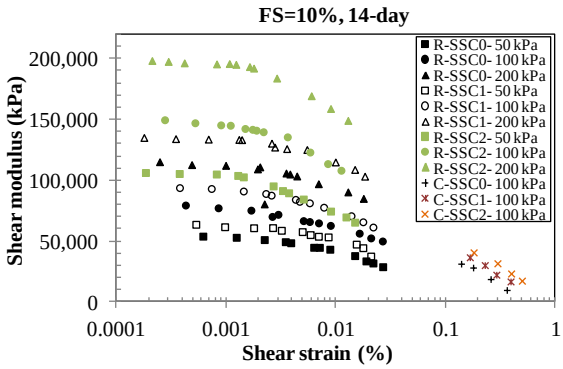


(d) FS=10%, 14-day

*Fig. 9. Shear modulus versus shear strain R-resonant column test C-cyclic triaxial test*

Fig. 10 shows the maximum shear modulus, $G_{max}$, for different grout contents. For SSC-0, the specimen of 10% FS has the higher $G_{max}$ than that of 0% FS, irrespective of confining pressure. In general, the grouted specimen has higher $G_{max}$ than non-grouted specimen, except the specimen of 10% FS at curing 3-day. Up to 1.25 - 1.96 increasing in $G_{max}$ of SSC-2 are obtained as comparing with that of SSC-0. When confining pressure increases, the Gmax increase. For example, when confining pressure increases from 50 to 100 kPa, the increment of Gmax is from 1.27 to 1.50 times, and the value in range from 1.82 to 2.18 times for confining pressure from 100 kPa to 200 kPa. In addition, increasing the curing time also increases the $G_{max}$. For instance, the increase of $G_{max}$ for SSC-1, SSC-2 are in range of 1.18 to 1.33 times, 1.44 - 1.67 times as curing days increases from 3-day to 14-day.

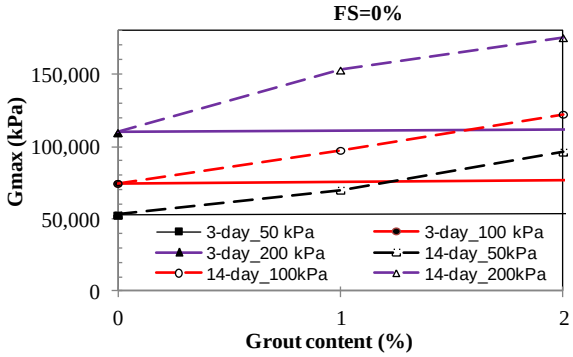


(a) FS=0%

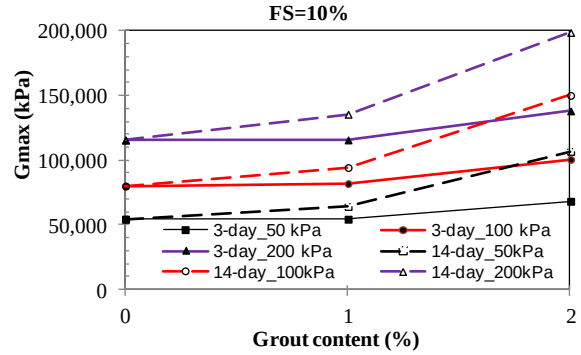


(b) FS=10%

*Fig. 10. Maximum shear modulus versus shear strain*

**5.2.2. Damping ratio:**

Resonant column test used to determine the damping ratio. The resonant frequency was applied, and thereafter, the excitation was suddenly to turn off, and the specimen was subjected to free oscillation. The damping ratio was determined depending on the free-vibration curve by the logarithmic decrement method [21].

$$D(\%) = \frac{1}{2\pi n} \ln\left(\frac{A_0}{A_n}\right) \qquad (3)$$

where A0 is the vibration amplitude of the first cycle after the excitation has been turned off; An is the vibration amplitude of the nth cycle; and n is the number of cycles in free vibration. The different results of damping ratio are expressed in Fig. 11(a)-(d). The insignificant.

results reveal that damping ratio nonlinearly increases with the increase in shear strain. The main reason can be explained that increase in damping ratios is caused by energy absorption because of particle rearrangement. The results show that the variation in the confining stress has a negligible effect on the damping ratio of sand and grouted sand, whatever the grout content. The results also meet in the agreement with [10, 22]. In addition, damping ratio of grouted sands is greater than that of non-grouted sand with the amplitude of strain in range of 0.001% and 0.1%. However, with the amplitude of strain greater than 0.1%, damping ratio of non-grouted-sand is greater than that of grouted-sand. Finally, the difference of damping ratio between curing 3- and 14-day is found

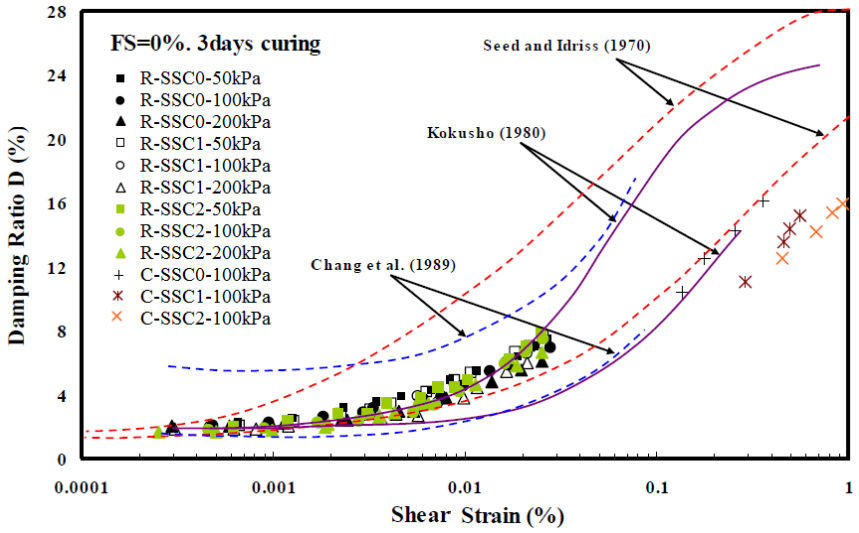


(a) FS=0%, 3-day

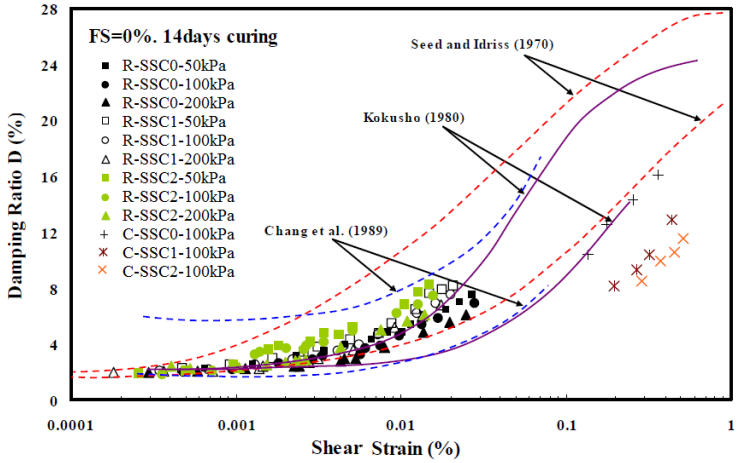


(b) FS=10%, 14-day

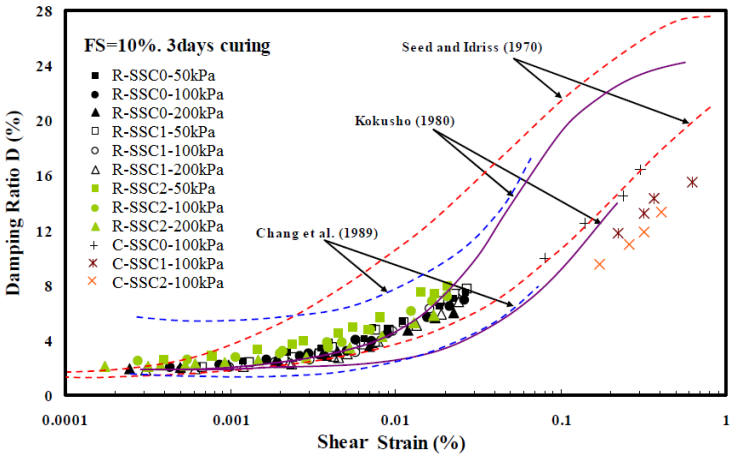


(c) FS=10%, 3-day

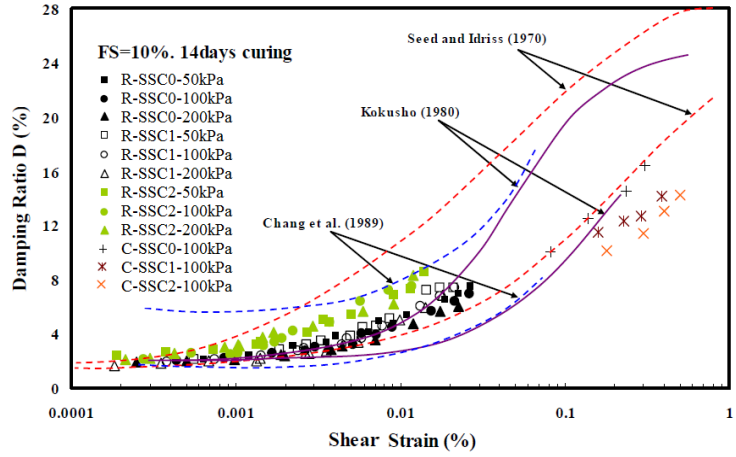


(d) FS=10%, 14-day

*Fig. 11. Damping ratio versus shear strain*

**6. Conclusions:**

The liquefaction resistance, shear modulus and damping ratio of pure sand and various grouted sands were determined using cyclic triaxial and resonant column tests. The effects of fine sand content, grout content, curing day, shear strain on the liquefaction resistance, shear modulus and the damping ratio were investigated. Based on the obtained results, the following conclusions can be drawn:

1. Fine sand content contributed the increasing the liquefaction resistance and shear modulus due to the well distribution grain size.
2. Liquefaction resistance increased with the increasing grout content and curing time. The CSR-grout content relation can be analytically expressed in an exponential function. Both axial strain and PWP described the different behavior between pure sand and grouted sands.
3. Variation of the confining pressure has a negligible effect on the damping ratio of pure sand and grouted sand, whatever the grout content.
4. Damping ratio of grouted sands is greater than that of pure sand with the amplitude of strain in range of 0.001% and 0.1%; however, with the amplitude of strain greater than 0.1%, the result is contrary. Finally, the difference of damping ratio between curing 7- and 14-day is found insignificant.

**7. References:**

[1] Maher MH, Ro KS, Welsh JP. Cyclic Undrained Behavior and Liquefaction Potential of Sand Treated with Chemical Grouts and Microfine Cement (MC-500). Geotechnical Testing Journal. 1994;17(2):159-70.

[2] Saxena SK, Reddy KR, Avramidis AS. Dynamic Behavior of Artificially Cemented Sands. Proceedings of Ninth World Conference on Earthquake Enginneering. Tokyo-Kyoto, Japan1988. p. 41-6.

[3] Tsai PH, Ni SH. Effects of Types of Additives on Dynamic properties of Cement Stabilized Soils.

International Journal of Applied Science and Engineering. 2012;10(2):131-44.
[4] Haeri SM, Hosseini SM, Toll DG, Yasrebi SS. The behaviour of an artificially cemented sandy gravel. Geotechnical and Geological Engineering. 2005;23(5):537-60.
[5] Dupas JM, Pecker A. Static and Dynamic properties of Sand-Cement. Journal of Geotechnical Engineering Division, ASCE. 1979;105(3):419-36.
[6] Chen JW, Lin CY. Cemented Behavior of Hydraulic Fill Material. The thirteenth (2003) International Offshore and polar Engineering Conference. Honolulu, Hawaii, USA 2003. p. 432-9.
[7] Acar YB, El-Tahir A. Low Strain Dynimic Properties of Artificially Cemented Sand. Journal of Geotechnical Engineering, ASCE. 1986;112(11):1001-15.
[8] Mollamahmutoglu M, Yilmaz Y. Engineering properties of medium-to-fine sands injected with microfine cement grout. Marine Georesources and Geotechnology. 2011;29(2):95-109.
[9] Mollamahmutoglu M, Yilmaz Y, Kutlu I. Grouting performance of microfine cement and sodium silica fume mix into sands. Journal of ASTM Internatinal. 2007;4(4):1-7.
[10] Delfosse-Ribay E, Djeran-Maigre I, Cabrillac R, Gouvenot D. Shear modulus and damping ratio of grouted sand. Soil Dynamics and Earthquake Engineering. 2004;24(6):461-71.
[11] Pantazopoulos IA, Atmatzidis DK. Dynamic properties of microfine cement grouted sands. Soil Dynamics and Earthquake Engineering. 2012;42:17-31.
[12] Gallagher PM, Mitchell JK. Influence of colloidal silica grout on liquefaction potential and cyclic undrained behavior of loose sand. Soil Dynamics and Earthquake Engineering. 2002;22(9–12):1017-26.
[13] Liao HJ, Huang CC, Chao BS. Liquefaction Resistance of a Colloid Silica Grouted Sand. Grouting and Ground Treatment. New Orleans, Louisiana, USA 2004. p. 1305-13.
[14] Persoff P, Apps J, Moridis G, Whang J. Effect of Dilution and Contaminants on Sand Grouted with Colloidal Silica. Journal of Geotechnical and Geoenvironmental Engineering. 1999;125(6):461-9.
[15] Yonekura R, Miwa M. Fundamental properties of sodium silicate based grout. Eleventh southeast Asia Geotechnical Conference, Singapore1993. p. 439-44.
[16] Kazemian S, Prasad A, Huat BBK, Ghiasi V, Ghareh S. Effects of Cement–Sodium Silicate System Grout on Tropical Organic Soils. Arab J Sci Eng. 2012;37(8):2137-48.
[17] Vipulanandan C, Ata A. Cyclic and Damping Properties of Silicate-Grouted Sand. Journal of Geotechnical and Geoenvironmental Engineering. 2000;126(7):650-6.
[18] Chang T, Woods R. Effect of confining pressure on shear modulus of cemented sand. Soil structure interaction. 1987:193-208.
[19] Taylor HFW. Cement Chemistry. 2nd Edition ed. Thomas Telford.1998.
[20] Chun BS, Yang HC, Park DH, Jung HS. Chemical and Physical Factors Influencing Behavior of Soidum Silicate-Cement Grout. The Eighteenth International Offshore and Polar Engineering Conference. Vancouver, BC, Canada2008. p. 821-7.
[21] Das BM, Ramana GV. Principles of Soil Dynamics. 2rd ed: Cengage Learning; 2010.
[22] Maher MH, Ro KS, Welsh JP. High strain dynamic modulus and damping of chemically grouted sand. Soil Dynamics and Earthquake Engineering. 1994;13(2):131-8.